MethodsX 10 (2023) 102116

Contents lists available at ScienceDirect

MethodsX

journal homepage: www.elsevier.com/locate/mex

Method Article

Modeling brain-heart interactions from Poincaré plot-derived measures of sympathetic-vagal activity

Diego Candia-Rivera

Paris Brain Institute (ICM), Sorbonne Université, CNRS UMR 7225, Inserm U1127, AP-HP Hôpital Pitié-Salpêtrière Paris, France

A R T I C L E I N F O

Method name:
Poincaré Sympathetic-Vagal Synthetic Data Generation (PSV-SDG)

Keywords:
Brain-heart interaction
Physiological modeling
Synthetic data generation
Heart rate variability

A B S T R A C T

Recent studies suggest that the interaction between the brain and heart plays a key role in cognitive processes, and measuring these interactions is crucial for understanding the interaction between the central and autonomic nervous systems. However, studying this bidirectional interplay presents methodological challenges, and there is still much room for exploration. This paper presents a new computational method called the Poincaré Sympathetic-Vagal Synthetic Data Generation Model (PSV-SDG) for estimating brain-heart interactions. The PSV-SDG combines EEG and cardiac sympathetic-vagal dynamics to provide time-varying and bidirectional estimators of mutual interplay. The method is grounded in the Poincaré plot, a heart rate variability method to estimate sympathetic-vagal activity that can account for potential non-linearities. This algorithm offers a new approach and computational tool for functional assessment of the interplay between EEG and cardiac sympathetic-vagal activity. The method is implemented in MATLAB under an open-source license.

- A new brain-heart interaction modeling approach is proposed.
- The modeling is based on coupled synthetic data generators of EEG and heart rate series.
- Sympathetic and vagal activities are gathered from Poincaré plot geometry.

Specifications table

Subject area:	Neuroscience
More specific subject area:	Autonomic Neuroscience
Name of your method:	Poincaré Sympathetic-Vagal Synthetic Data Generation (PSV-SDG)
Name and reference of original method:	First proposal to study heart rate variability with Poincaré plots, by Woo et al. [1] Modeling of heart rate oscillations using Poincaré plots, by Brennan et al. [2] Modeling of EEG signals using adaptive Markov process, by Al-Nashash et al. [3] Original proposal of brain-heart modeling through synthetic data generation models, by Catrambone et al. [4] Alternative proposal of brain-heart modeling through synthetic data generation models, by Candia-Rivera et al. [5]
Resource availability:	https://github.com/diegocandiar/brain_heart_psv_sdg

Introduction

Brain-heart interactions are actively involved in cognitive processes, such as perception, decision, and action [6]. Recently proposed methods for brain-heart interaction analysis exploit signal processing techniques to uncover these interactions, including inferences on causality and directionality between cortical and cardiac oscillations [7]. State-of-the-art methods of brain-heart interaction

E-mail address: diego.candia.r@ug.uchile.cl

https://doi.org/10.1016/j.mex.2023.102116
Received 5 November 2022; Accepted 6 March 2023
Available online 8 March 2023

include the analysis of heartbeat-contingent responses [8], convergent cross-mapping [9], coupling through symbolic representations [10], time-delay stability [11], granger causality [12], transfer entropy [13], among others. Synthetic Data Generation (SDG) modeling is a framework that aims to gather the bidirectional interactions of EEG and sympathetic-vagal activity [4,5]. The estimation of bidirectional interactions is done through a generative model of neural dynamics, where two physiologically-inspired models of synthetic EEG and heart rate series are coupled to gather the mutual interactions [6].

The analysis of brain-heart interaction aims to provide evidence on how the central nervous system interacts with the sympathetic and vagal branches of the autonomic nervous system [14]. However, current heart rate spectral analysis is challenged because such estimators do not allow a proper quantification of cardiac sympathetic activity. This is because sympathetic activity is typically studied in the 0.04–0.15 Hz range, which may also be affected by changes in vagal oscillations [15,16]. Additionally, using fixed frequency bands to study sympathetic and vagal activities may be inaccurate due to nonlinear fluctuations in heart rate variability. An alternative method is the use of Poincaré plots, which illustrate beat-to-beat changes in heart rate, accounting for nonlinearities and reflecting short- and long-term fluctuations of heart rate variability [1,17]. Poincaré plot-derived measures have been proposed as a potential methodology to gather sympathetic and vagal tone [18–20] and have shown to accurately describe changes in vagal and sympathetic tone in both healthy participants and pathological conditions [21–23].

Method details

The proposed method requires as inputs time-varying EEG power and interbeat interval (IBI) series gathered from ECG. Below is described the preprocessing of EEG and ECG series, used to validate the method.

EEG preprocessing

The EEG preprocessing involves frequency filtering, large artifact removal, eye movements, cardiac-field artifact removal, interpolation of contaminated electrodes, and common average reference, as detailed elsewhere [7]. EEG data were bandpass filtered with a Butterworth filter of order 4, between 0.5 and 45 Hz. Note that the proposed method requires continuous EEG power series. Therefore, to retain the EEG's entire length, adequate removal of large muscle artifacts is necessary. The proposed strategy used wavelet filtering on the independent component space. In brief, independent components analysis (ICA) was computed to identify large artifacts from the ICA series. Then, the ICA series were subjected to wavelet transform and thresholded to remove only the large artifacts [24]. The large artifact identification could be done with either automated thresholding or manually. Afterward, all the time series are combined to reconstruct the EEG series, and ICA was re-run to identify and remove physiological artifacts (eye movements and cardiac-field artifacts). Contaminated EEG channels were identified under two criteria: First, channels were marked as contaminated if their area under the curve exceeded three standard deviations of the mean of all electrodes. Second, channels were compared with their weighted-by-distance-correlation neighbors using the standard Fieldtrip neighbor's definition for 32 electrodes Biosemi system. If a channel resulted in a weighted-by-distance correlation coefficient of less than 0.5, it was considered contaminated. A maximum of 6 channels was imposed using the two criteria. Contaminated channels were replaced by the neighbor's interpolation, as implemented in Fieldtrip [25]. EEG channels were re-referenced offline using a common average [7].

The EEG spectrogram was computed using a short-time Fourier transform with a Hanning taper. The calculations were performed with a sliding time window of 2 s with a 50% overlap, resulting in a spectrogram resolution of 1 s and 0.5 Hz. Successively, time series were integrated within five frequency bands: delta (δ; 0–4 Hz), theta (θ; 4–8 Hz), alpha (α; 8–12 Hz), beta (β; 12–30 Hz) and gamma (γ; 30–45 Hz).

ECG preprocessing

The ECG preprocessing involves frequency filtering, R-peak detection, and correction of misdetections. ECG data were bandpass filtered using a Butterworth filter of order 4, between 0.5 and 45 Hz. Heartbeats from QRS waves were identified in an automated process based on a template-based method for detecting R-peaks [7]. Misdetections were corrected first by visual inspection of detected peaks and the respective inter-beat interval histogram. Note that automated algorithms for the detection of ectopic beats can be used as well [26].

Estimation of sympathetic and vagal activity from Poincaré plot

Poincaré plot is a non-linear method to study heart rate variability and depicts the fluctuations on the duration of consecutive IBI [17], as shown in Fig. 1. Different measures gathered from Poincaré plot geometry have been proposed to characterize changes on heart rate. The typically quantified features from Poincaré plot are the SD_1 and SD_2, the ratios of the ellipse formed from consecutive changes in IBIs, representing the short- and long-term fluctuations of heart rate variability, respectively [27].

The ellipse ratios for the whole experimental condition SD_{01} and SD_{02} are computed as follows:

$$SD_{01} = \sqrt{\frac{1}{2} std(IBI')^2} \tag{1}$$

$$SD_{02} = \sqrt{2 std(IBI)^2 - \frac{1}{2} std(IBI')^2} \tag{2}$$

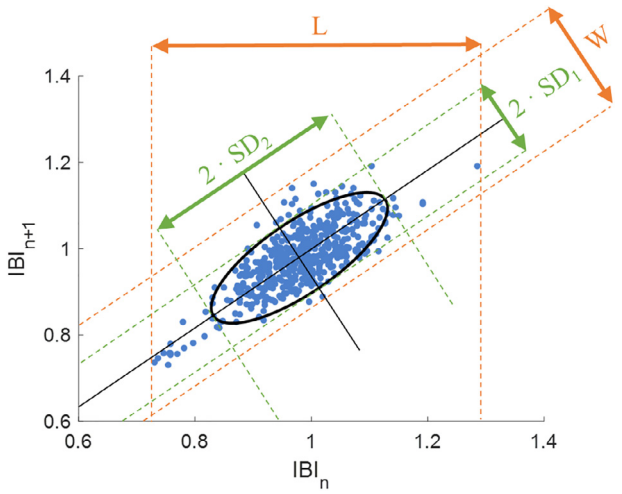

Fig. 1. Poincaré plot example. In green the geometric features used for the heart-to-brain model, corresponding to the standard deviation in both axes. In orange the geometric features used for the brain-to-heart model, corresponding to the length and width of the Poincaré plot.

where IBI' is the derivative of IBI and $std()$ refers to the standard deviation.

In this framework, I propose to study brain-heart interactions using the changes in time of the Poincaré ellipse. The time-varying fluctuations of the ellipse ratios are computed with a sliding-time window, as shown in Eqs. (3) and 4:

$$SD_1(t) = \sqrt{\frac{1}{2} std\left(IBI'_{\Omega_t}\right)^2} \tag{3}$$

$$SD_2(t) = \sqrt{2std\left(IBI_{\Omega_t}\right)^2 - \frac{1}{2} std\left(IBI'_{\Omega_t}\right)^2} \tag{4}$$

where $\Omega_t : t - T \leq t_i \leq t$, in this study T is fixed in 15 s.

The Cardiac Vagal Index (CVI), Sympathetic Index (CSI), and Sympathovagal balance Index (SVI) are computed as follows:

$$CVI(t) = SD_{01} + \overline{SD_1}(t) \tag{5}$$

$$CSI(t) = SD_{02} + \overline{SD_2}(t) \tag{6}$$

$$SVI(t) = CSI(t)/CVI(t) \tag{7}$$

where $\overline{SD_x}$ is the demeaned SD_x

Estimation of functional brain–heart interactions

Functional brain-heart interplay was estimated using the Poincaré Sympathovagal Synthetic Data Generation (PSV-SDG) model.

The interplay from the brain to the heart was quantified through a model of synthetic heartbeat intervals, based on an integral pulse frequency modulation model parameterized with Poincaré plot features [2]. The synthetic heartbeats were modeled as Dirac functions δ(t), as shown in Fig. 2. The heartbeats generation occurs at the timings t_k, as presented in Eq. (8). Heartbeat generation is triggered by the integral of a reference heart rate μ_{HR} and a modulation function $m(t)$, as shown in Eq. (9), where a new R-peak is generated when the integral function reaches a threshold value of 1.

$$x(t) = \sum_{k=1}^{N} \delta\left(t - t_k\right) \tag{8}$$

$$1 = \int_{t_k}^{t_{k+1}} \left[\mu_{HR} + m(t)\right] dt \tag{9}$$

Eq. (10) presents $m(t)$ as a sum of two oscillators representing the sympathetic and vagal autonomic outflows. The oscillators are centered at the frequencies ω_S and ω_V, with amplitudes defined by C_S and C_V, representing the sympathetic and vagal activities, respectively.

$$m(t) = C_S(t) \cdot sin\left(\omega_S t\right) + C_V(t) \cdot sin\left(\omega_V t\right) \tag{10}$$

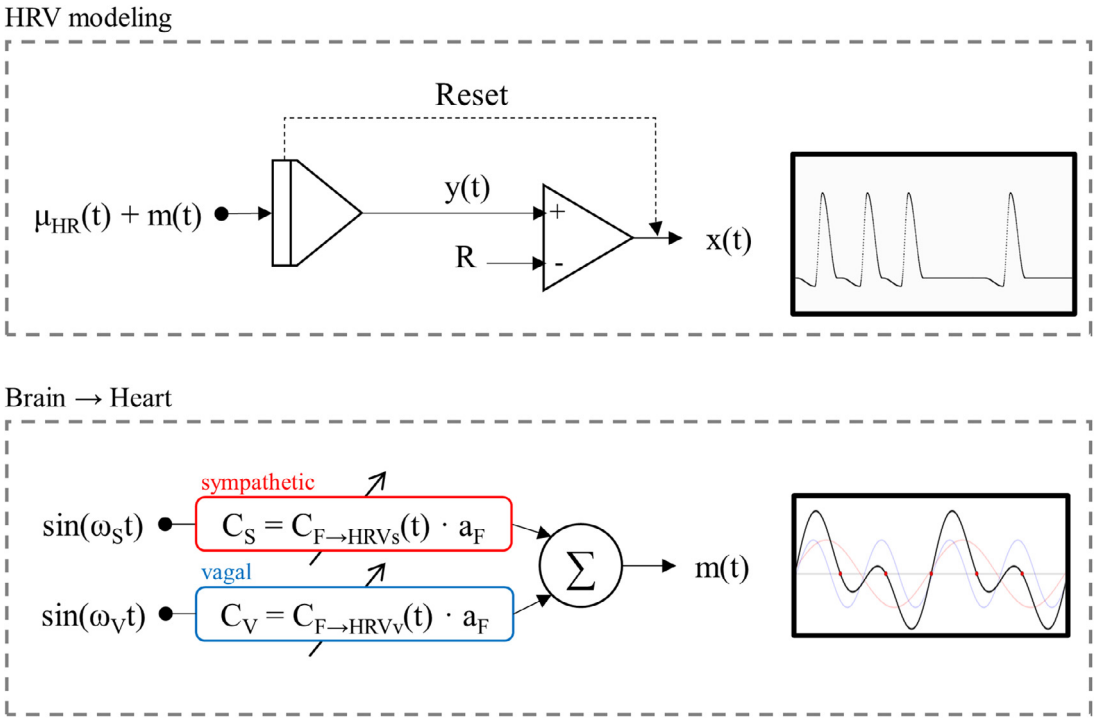

Fig. 2. Heart rate variability (HRV) modeling and the brain-to-heart estimation schematic.

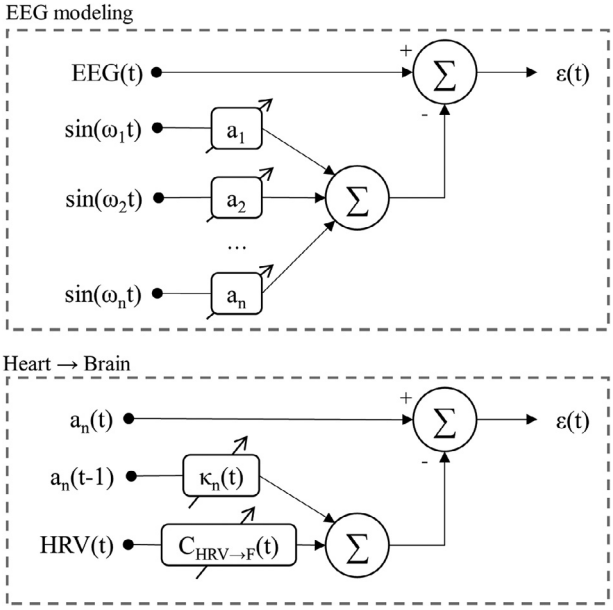

Fig. 3. EEG modeling and the heart-to-brain estimation schematic.

C_S and C_V are computed as a function of heart rate variability. In brief, the parameters L and W are the length and width of the Poincaré Plot, as shown in Fig. 1:

$$L = \max_k IBI_k - \min_k IBI_k \tag{11}$$

$$W = \sqrt{2}\max_k \{IBI_k - IBI_{k-1}\} \tag{12}$$

Table 1
Trials studied, divided in pleasant and unpleasant. Trial numbers correspond to the assigned identification in the dataset. Values reported for valence and arousal correspond to the group median ($N = 32$).

Pleasant trials (high arousal and high valence)										
Trial:	1	3	4	8	9	11	14	18	19	20
Valence:	7	7.5	7	7.1	7.1	7.3	8	7.3	7.3	7
Arousal:	5.8	6.7	6	5.7	6	5.7	5	5	6.1	5.8
Unpleasant trials (high arousal and low valence)										
Trial:	24	30	31	32	34	35	36	37	38	39
Valence:	3.3	3.1	4	4	4.1	3.1	3.9	3	2.2	3.2
Arousal:	5	6	6	7	6.4	6	6.6	6.1	6.2	6.2

Table 2
Video clip excerpts of the trials studied, divided in pleasant and unpleasant.

Pleasant trials (high arousal and high valence)		
1	Emilíana Torrini	Jungle Drum
3	Jackson 5	Blame It On The Boogie
4	The B52′S	Love Shack
8	Lily Allen	F— You
9	Queen	I Want To Break Free
11	Michael Franti & Spearhead	Say Hey (I Love You)
14	Jason Mraz	I'm Yours
18	Louis Armstrong	What A Wonderful World
19	Manu Chao	Me Gustas Tu
20	Taylor Swift	Love Story
Unpleasant trials (high arousal and low valence)		
24	James Blunt	Goodbye My Lover
30	Enya	May It Be (Saving Private Ryan)
31	Mortemia	The One I Once Was
32	Marilyn Manson	The Beautiful People
34	Dj Paul Elstak	A Hardcore State Of Mind
35	Napalm Death	Procrastination On The Empty Vessel
36	Sepultura	Refuse Resist
37	Cradle Of Filth	Scorched Earth Erotica
38	Gorgoroth	Carving A Giant
39	Dark Funeral	My Funeral

These parameters can be estimated as a function of the heart rate, using trigonometric identities and mathematical approximations, as described in [2]:

$$L \approx \frac{4}{\mu_{HR}}\left[\frac{C_S}{\omega_S}\left|sin\left(\frac{\omega_S}{2\mu_{HR}}\right)\right| + \frac{C_V}{\omega_V}\left|sin\left(\frac{\omega_V}{2\mu_{HR}}\right)\right|\right] \tag{13}$$

$$W \approx \frac{4\sqrt{2}}{\mu_{HR}}\left[\frac{C_S}{\omega_S}sin^2\left(\frac{\omega_S}{2\mu_{HR}}\right) + \frac{C_V}{\omega_V}sin^2\left(\frac{\omega_V}{2\mu_{HR}}\right)\right] \tag{14}$$

Therefore, by resolving the system of Eqs. (13) and (14), C_S and C_V are computed as follows:

$$\begin{bmatrix} C_S \\ C_V \end{bmatrix} = \frac{1}{\gamma}\begin{bmatrix} \frac{\sin(\omega_p/2\mu_{HR})\omega_s\mu_{HR}}{4\ \sin(\omega_s/2\mu_{HR})} & \frac{-\sqrt{2}\omega_s\ \mu_{HR}}{8\ \sin(\omega_s/2\mu_{HR})} \\ \frac{-\sin(\omega_s\ /2\mu_{HR})\omega_p\mu_{HR}}{4\ \sin(\omega_p/2\mu_{HR})} & \frac{\sqrt{2}\omega_p\mu_{HR}}{8\ \sin(\omega_p/2\mu_{HR})} \end{bmatrix}\begin{bmatrix} L \\ W \end{bmatrix} \tag{15}$$

$$\gamma = sin(\omega_p/2\mu_{HR}) - sin(\omega_s/2\mu_{HR}) \tag{16}$$

Finally, the brain to heart interaction coefficients are quantified as the ratio between C_S and C_V, and the EEG power in the frequency $F(i.e.,\ \delta,\ \theta,\ \alpha,\ \beta,\ or\ \gamma)$, during the previous time window $a_F(t-1)$. Eqs. (12) and (13) present the final computation of the brain-to-sympathetic and brain-to-vagal interplay coefficients $C_{F\rightarrow CSI}$ and $C_{F\rightarrow -CVI}$, respectively.

$$C_{F\rightarrow CSI}(t) = C_S(t)/\ a_F(t-1) \tag{12}$$

$$C_{F\rightarrow CVI}(t) = C_V(t)/\ a_F(t-1) \tag{13}$$

The interplay from the heart to the brain is quantified through a model based of synthetic EEG series using an adaptive Markov process [3]. The changes on EEG are modelled as fluctuations in EEG power at different frequency bands, as shown in Fig. 3 and Eq. (14), where f is the main frequency in a defined frequency band, and θ_f is the phase. The changes in the EEG power are modelled

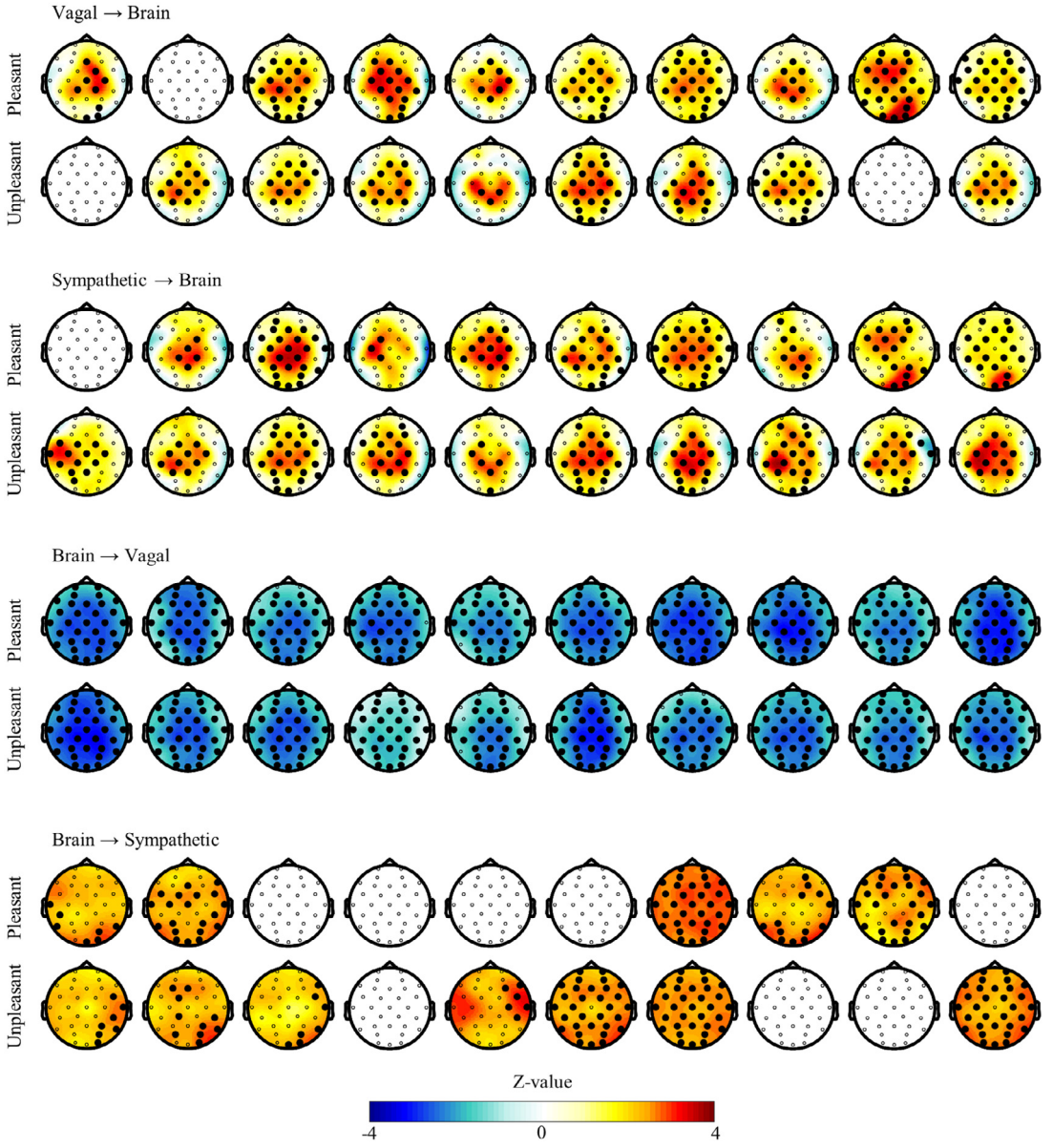

Fig. 4. Brain-heart model validation in emotion elicitation. The test is performed on 20 trials of emotion elicitation, 10 pleasant and 10 unpleasant trials. The displayed results correspond to the clustered effects found in the 3D space (time-frequency-channel) when comparing emotion elicitation vs rest. Colormaps represent the Z-value from the Wilcoxon test performed and thick channels indicate clustered effect at $p < 0.001$ after permutation.

by the coefficient Ψ_f using least squares in an exogenous autoregressive process, as shown in Eq. (15), κ_f is a constant, and ε_f is a Gaussian white noise term.

$$EEG(t) = \sum_{f=f_1}^{f_n} a_f(t) \cdot \sin\left(\omega_f t + \theta_f\right) \tag{14}$$

$$a_f(t) = \kappa_f \cdot a_f(t-1) + \Psi_f(t-1) + \varepsilon_f \tag{15}$$

The Markovian neural activity generation uses its previous neural activity and heartbeat dynamics as inputs for EEG data generation. The coefficients $C_{CSI \to F}$ and $C_{CVI \to F}$ can be modelled from the contribution of heartbeat dynamics and the exogenous term of the autoregressive model, as follows:

$$C_{CSI \to F}(t) = \Psi_F(t) \,/\, CSI(t) \tag{16}$$

$$C_{CVI \to F}(t) = \Psi_F(t) \,/\, CVI(t) \tag{17}$$

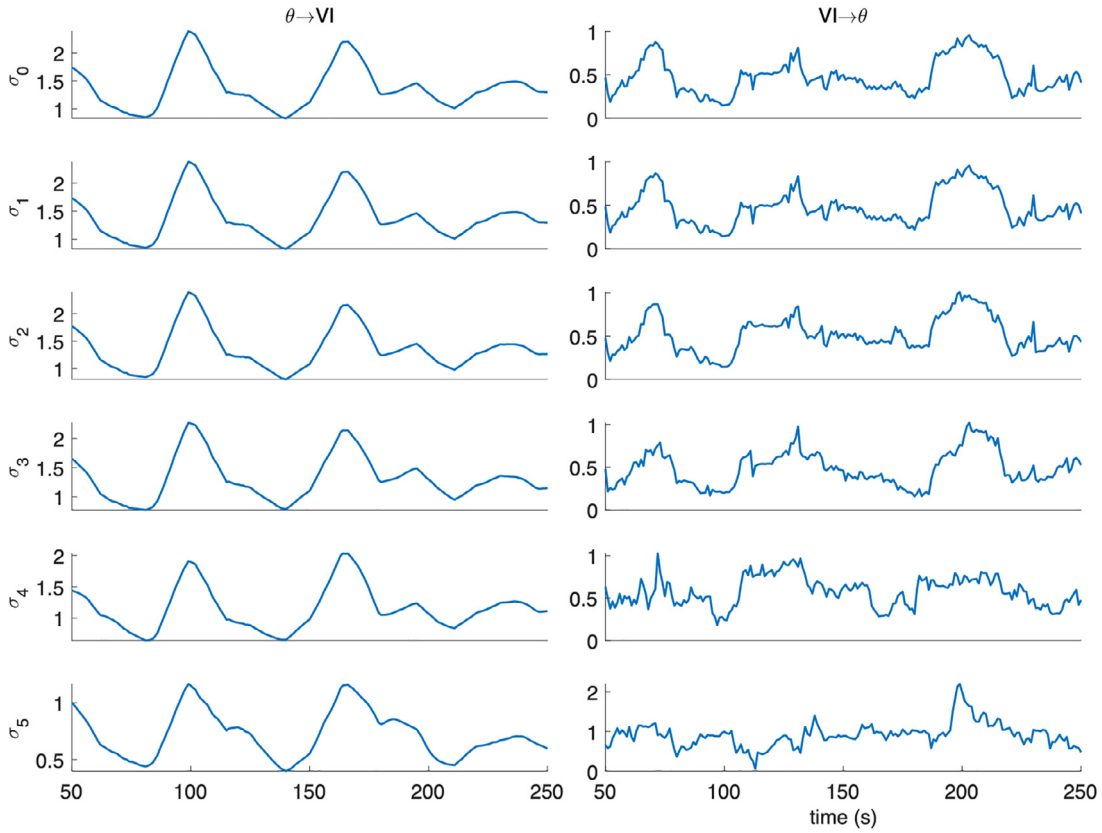

Fig. 5. Brain-heart coupling coefficients obtained from generated EEG and HRV data, for the interplay between vagal index (VI) and theta. Each row corresponds to the coupling coefficients computed for different levels of noise in EEG data. The noise standard deviations are $\sigma i = \{0\ 0.5\ 1\ 2\ 4\}$.

For this study, the model computed the coefficients using a 15 s long time window with a 1 s step to estimate the coefficients. The central frequencies used were $\omega_S = 2\pi \cdot 0.1 rad/s$ and $\omega_V = 2\pi \cdot 0.25 rad/s$, in which 0.1 Hz and 0.25 Hz correspond to sympathetic and vagal frequencies, respectively.

For the statistical comparison of the computed biomarkers, nonparametric statistics are recommended [28].

Method validation

The method validation was performed over an open dataset of emotion elicitation [29]. The dataset comprises healthy human volunteers undergoing audiovisual stimulations with affective content. The dataset consists of 32 subjects (age range, 19–27 years; median, 27 years; 16 females) visualizing 40 one-minute video clips. Videos were presented after an initial resting period of two-minute and separated by a pad of 5 s. Subjective ratings of arousal and valence were reported by participants, from 1 to 9. Physiological data includes 32-channel EEG and ECG, sampled at 512 Hz.

A total of 20 trials were selected for the method validation procedure. 10 trials with high arousal and high valence were labeled as pleasant trials, and 10 trials with high arousal and low valence were labeled as unpleasant trials. Details on the selected trials in this study are displayed on Tables 1 and 2.

Brain-heart interaction estimators were computed using the proposed method PSV-SDG for the whole experimental condition. Statistical comparisons were performed between each trial and the averaged resting state period. The statistical comparison was performed using a nonparametric cluster permutation analysis on a 3D space (time-frequency-channel) [28], separately for sympathetic-vagal interplay and directionality. Therefore, each trial was compared against the initial resting state in sympathetic-to-brain, vagal-to-brain, brain-to-sympathetic, and brain-to-vagal.

Results shown in Fig. 4 depict that brain-heart interaction estimators distinguish rest from emotion elicitation in most of the selected trials.

As an additional method of validation, synthetic EEG and HRV data were generated to depict the parallel fluctuations in time of the brain-heart interplay. HRV data was initialized from a white noise signal, from uniformly distributed random numbers between 0 and 1, and then standardized to 100 ms and mean 700 ms. EEG data was generated at 256 Hz sampling frequency as a sum of five oscillators at 2, 6, 10, 20, and 40 Hz. The time-varying oscillator amplitudes were initially generated as white noise and then imposed

as an autoregressive process of order 1. White noise was added to the simulated EEG data at 0.5, 1, 2, and 4 standard deviations. PSV-SDG coupling coefficients were computed from the generated data. Fig. 5 shows the simulation results for the interplay between the cardiac vagal index and theta oscillations. The top row shows the ascending and descending coupling coefficients on time without added noise, and the rows below correspond to the different levels of added noise. The results on the effects of the level of noise on the coupling estimation show that descending interplay coefficients are not much affected. However, ascending interplay with added noise at $\sigma = 4$ shows that the estimated coupling coefficients qualitatively differ from the lower noise levels. Previous simulations in other models of brain-heart interplay using synthetic data generation models showed similar results, where low noise levels do not affect the brain-heart interplay estimation [4,5].

The interactions between the brain and peripheral organs are linked to different neural pathways, including visceral, pain, and thalamocortical pathways [30]. Overlapping brain regions control autonomic pathways for the activity of peripheral organs with sensory specificity [31]. The high integration in network physiology mechanisms shows the importance of modeling interoceptive processes to understand multisystem dysfunctions [14]. The importance of the study of brain-heart interactions is supported by previous research showing the involvement of heartbeat dynamics in several cognitive processes, including emotions [32] and self-awareness [33,34]. The characterization of functional brain-heart interactions has contributed to the development of novel biomarkers with potential clinical use [9,35–40]. The proposed method has the advantage of assessing the directionality and latencies of functional brain-heart interactions, with numerous neuroscientific and clinical applications.

Ethics statements

The method validation was performed on open data, consisting in non-invasive physiological recordings from human volunteers [29]. All participants signed a consent form to participate in the study, as required by the declaration of Helsinki.

Declaration of Competing Interest

The authors declare that they have no known competing financial interests or personal relationships that could have appeared to influence the work reported in this paper.

CRediT authorship contribution statement

Diego Candia-Rivera: Conceptualization, Methodology, Software, Investigation, Writing – original draft.

Data availability

The data used is publicly available.

Acknowledgments

This research did not receive any specific grant from funding agencies in the public, commercial, or not-for-profit sectors.

The founding source reported in the open dataset used for the method validation is European Community's 17th Framework Program (FP7/2007-2011) under grant agreement No. 216444 (PetaMedia) [29].

References

[1] M.A. Woo, W.G. Stevenson, D.K. Moser, R.B. Trelease, R.M. Harper, Patterns of beat-to-beat heart rate variability in advanced heart failure, Am. Heart J. 123 (1992) 704–710, doi:10.1016/0002-8703(92)90510-3.
[2] M. Brennan, M. Palaniswami, P. Kamen, Poincaré plot interpretation using a physiological model of HRV based on a network of oscillators, Am. J. Physiol. Heart Circ. Physiol. 283 (2002) H1873–H1886, doi:10.1152/ajpheart.00405.2000.
[3] H. Al-Nashash, Y. Al-Assaf, J. Paul, N. Thakor, EEG signal modeling using adaptive Markov process amplitude, IEEE Trans. Biomed. Eng. 51 (2004) 744–751, doi:10.1109/TBME.2004.826602.
[4] V. Catrambone, A. Greco, N. Vanello, E.P. Scilingo, G. Valenza, Time-resolved directional brain-heart interplay measurement through synthetic data generation models, Ann. Biomed. Eng. 47 (2019) 1479–1489, doi:10.1007/s10439-019-02251-y.
[5] D. Candia-Rivera, V. Catrambone, R. Barbieri, G. Valenza, Functional assessment of bidirectional cortical and peripheral neural control on heartbeat dynamics: a brain-heart study on thermal stress, Neuroimage 251 (2022) 119023, doi:10.1016/j.neuroimage.2022.119023.
[6] D. Candia-Rivera, Brain-heart interactions in the neurobiology of consciousness, Curr. Res. Neurobiol. 3 (2022) 100050, doi:10.1016/j.crneur.2022.100050.
[7] D. Candia-Rivera, V. Catrambone, G. Valenza, The role of electroencephalography electrical reference in the assessment of functional brain–heart interplay: from methodology to user guidelines, J. Neurosci. Methods 360 (2021) 109269, doi:10.1016/j.jneumeth.2021.109269.
[8] H.D. Park, O. Blanke, Heartbeat-evoked cortical responses: underlying mechanisms, functional roles, and methodological considerations, Neuroimage 197 (2019) 502–511, doi:10.1016/j.neuroimage.2019.04.081.
[9] K. Schiecke, A. Schumann, F. Benninger, M. Feucht, K.J. Baer, P. Schlattmann, Brain-heart interactions considering complex physiological data: processing schemes for time-variant, frequency-dependent, topographical and statistical examination of directed interactions by convergent cross mapping, Physiol. Meas. 40 (2019) 114001, doi:10.1088/1361-6579/ab5050.
[10] M. Dumont, F. Jurysta, J.P. Lanquart, P.F. Migeotte, P. van de Borne, P. Linkowski, Interdependency between heart rate variability and sleep EEG: linear/non-linear? Clin. Neurophysiol. 115 (2004) 2031–2040, doi:10.1016/j.clinph.2004.04.007.
[11] A. Bashan, R.P. Bartsch, J.W. Kantelhardt, S. Havlin, P.C. Ivanov, Network physiology reveals relations between network topology and physiological function, Nat. Commun. 3 (2012) 702, doi:10.1038/ncomms1705.
[12] L. Faes, G. Nollo, A. Porta, Information-based detection of nonlinear Granger causality in multivariate processes via a nonuniform embedding technique, Phys. Rev. E 83 (2011) 051112, doi:10.1103/PhysRevE.83.051112.

[13] M. Kumar, D. Singh, K.K. Deepak, Identifying heart-brain interactions during internally and externally operative attention using conditional entropy, Biomed. Signal Process. Control 57 (2020) 101826, doi:10.1016/j.bspc.2019.101826.
[14] W.G. Chen, D. Schloesser, A.M. Arensdorf, J.M. Simmons, C. Cui, R. Valentino, J.W. Gnadt, L. Nielsen, C.S. Hillaire-Clarke, V. Spruance, T.S. Horowitz, Y.F. Vallejo, H.M. Langevin, The emerging science of interoception: sensing, integrating, interpreting, and regulating signals within the self, Trends Neurosci. 44 (2021) 3–16, doi:10.1016/j.tins.2020.10.007.
[15] G.A. Reyes del Paso, W. Langewitz, L.J.M. Mulder, A. van Roon, S. Duschek, The utility of low frequency heart rate variability as an index of sympathetic cardiac tone: a review with emphasis on a reanalysis of previous studies, Psychophysiology 50 (2013) 477–487, doi:10.1111/psyp.12027.
[16] Task Force of the European Society of Cardiology the North American Society of Pacing, Heart rate variability: standards of measurement, physiological interpretation, and clinical use, Circulation 93 (1996) 1043–1065, doi:10.1161/01.CIR.93.5.1043.
[17] M. Brennan, M. Palaniswami, P. Kamen, Do existing measures of Poincare plot geometry reflect nonlinear features of heart rate variability? IEEE Trans. Biomed. Eng. 48 (2001) 1342–1347, doi:10.1109/10.959330.
[18] S. Rahman, M. Habel, R.J. Contrada, Poincaré plot indices as measures of sympathetic cardiac regulation: responses to psychological stress and associations with pre-ejection period, Int. J. Psychophysiol. 133 (2018) 79–90, doi:10.1016/j.ijpsycho.2018.08.005.
[19] D. Petković, Ž. Ćojbašić, Adaptive neuro-fuzzy estimation of autonomic nervous system parameters effect on heart rate variability, Neural Comput. Appl. 21 (2012) 2065–2070, doi:10.1007/s00521-011-0629-z.
[20] C.K. Karmakar, A.H. Khandoker, J. Gubbi, M. Palaniswami, Complex correlation measure: a novel descriptor for Poincaré plot, Biomed. Eng. Online 8 (2009) 17, doi:10.1186/1475-925X-8-17.
[21] P. Contreras, R. Canetti, E.R. Migliaro, Correlations between frequency-domain HRV indices and lagged Poincaré plot width in healthy and diabetic subjects, Physiol. Meas. 28 (2006) 85–94, doi:10.1088/0967-3334/28/1/008.
[22] G. De Vito, S. d. r. Galloway, M.A. Nimmo, P. Maas, J.J.V. McMurray, Effects of central sympathetic inhibition on heart rate variability during steady-state exercise in healthy humans, Clin. Physiol. Funct. Imaging 22 (2002) 32–38, doi:10.1046/j.1475-097X.2002.00395.x.
[23] R.A. Hoshi, C.M. Pastre, L.C.M. Vanderlei, M.F. Godoy, Poincaré plot indexes of heart rate variability: relationships with other nonlinear variables, Auton. Neurosci. 177 (2013) 271–274, doi:10.1016/j.autneu.2013.05.004.
[24] L.J. Gabard-Durnam, A.S. Mendez Leal, C.L. Wilkinson, A.R. Levin, The harvard automated processing pipeline for electroencephalography (HAPPE): standardized processing software for developmental and high-artifact data, Front. Neurosci. 12 (2018), doi:10.3389/fnins.2018.00097.
[25] R. Oostenveld, P. Fries, E. Maris, J.M. Schoffelen, FieldTrip: open source software for advanced analysis of MEG, EEG, and invasive electrophysiological data, Comput. Intell. Neurosci. 2011 (2011) 9, doi:10.1155/2011/156869.
[26] L. Citi, E.N. Brown, R. Barbieri, A real-time automated point process method for detection and correction of erroneous and ectopic heartbeats, IEEE Trans. Biomed. Eng. 59 (2012) 2828–2837, doi:10.1109/TBME.2012.2211356.
[27] R. Sassi, S. Cerutti, F. Lombardi, M. Malik, H.V. Huikuri, C.K. Peng, G. Schmidt, Y. Yamamoto, D. Reviewers, B. Gorenek, G.Y.H. Lip, G. Grassi, G. Kudaiberdieva, J.P. Fisher, M. Zabel, R. Macfadyen, Advances in heart rate variability signal analysis: joint position statement by the e-cardiology ESC working group and the European heart rhythm association co-endorsed by the asia pacific heart rhythm society, Europace 17 (2015) 1341–1353, doi:10.1093/europace/euv015.
[28] D. Candia-Rivera, G. Valenza, Cluster permutation analysis for EEG series based on non-parametric Wilcoxon–Mann–Whitney statistical tests, SoftwareX 19 (2022) 101170, doi:10.1016/j.softx.2022.101170.
[29] S. Koelstra, C. Muhl, M. Soleymani, J.S. Lee, A. Yazdani, T. Ebrahimi, T. Pun, A. Nijholt, I. Patras, DEAP: a database for emotion analysis ;using physiological signals, IEEE Trans. Affect. Comput. 3 (2012) 18–31, doi:10.1109/T-AFFC.2011.15.
[30] A.D. Craig, How do you feel? Interoception: the sense of the physiological condition of the body, Nat. Rev. Neurosci. 3 (2002) 655–666, doi:10.1038/nrn894.
[31] I. Rebollo, A.D. Devauchelle, B. Béranger, C. Tallon-Baudry, Stomach-brain synchrony reveals a novel, delayed-connectivity resting-state network in humans, Elife 7 (2018) e33321, doi:10.7554/eLife.33321.
[32] D. Candia-Rivera, V. Catrambone, J.F. Thayer, C. Gentili, G. Valenza, Cardiac sympathetic-vagal activity initiates a functional brain–body response to emotional arousal, Proc. Natl. Acad. Sci. 119 (2022) e2119599119, doi:10.1073/pnas.2119599119.
[33] H.D. Park, F. Bernasconi, J. Bello-Ruiz, C. Pfeiffer, R. Salomon, O. Blanke, Transient modulations of neural responses to heartbeats covary with bodily self-consciousness, J. Neurosci. 36 (2016) 8453–8460, doi:10.1523/JNEUROSCI.0311-16.2016.
[34] M. Babo-Rebelo, C.G. Richter, C. Tallon-Baudry, Neural responses to heartbeats in the default network encode the self in spontaneous thoughts, J. Neurosci. 36 (2016) 7829–7840, doi:10.1523/JNEUROSCI.0262-16.2016.
[35] V. Catrambone, S. Messerotti Benvenuti, C. Gentili, G. Valenza, Intensification of functional neural control on heartbeat dynamics in subclinical depression, Transl. Psychiatry 11 (2021) 1–10, doi:10.1038/s41398-021-01336-4.
[36] D. Candia-Rivera, J. Annen, O. Gosseries, C. Martial, A. Thibaut, S. Laureys, C. Tallon-Baudry, Neural responses to heartbeats detect residual signs of consciousness during resting state in postcomatose patients, J. Neurosci. 41 (2021) 5251–5262, doi:10.1523/JNEUROSCI.1740-20.2021.
[37] T.A. Iseger, F. Padberg, J.L. Kenemans, H. van Dijk, M. Arns, Neuro-cardiac-guided TMS (NCG TMS): a replication and extension study, Biol. Psychol. 162 (2021) 108097, doi:10.1016/j.biopsycho.2021.108097.
[38] L. Perogamvros, H.D. Park, L. Bayer, A.A. Perrault, O. Blanke, S. Schwartz, Increased heartbeat-evoked potential during REM sleep in nightmare disorder, Neuroimage Clin. 22 (2019) 101701, doi:10.1016/j.nicl.2019.101701.
[39] J. Terhaar, F.C. Viola, K.J. Bär, S. Debener, Heartbeat evoked potentials mirror altered body perception in depressed patients, Clin. Neurophysiol. 123 (2012) 1950–1957, doi:10.1016/j.clinph.2012.02.086.
[40] P.C. Salamone, A. Legaz, L. Sedeño, S. Moguilner, M. Fraile-Vazquez, C.G. Campo, S. Fittipaldi, A. Yoris, M. Miranda, A. Birba, A. Galiani, S. Abrevaya, A. Neely, M.M. Caro, F. Alifano, R. Villagra, F. Anunziata, M.O. de Oliveira, R.M. Pautassi, A. Slachevsky, C. Serrano, A.M. García, A. Ibañez, Interoception primes emotional processing: multimodal evidence from neurodegeneration, J. Neurosci. 41 (2021) 4276–4292, doi:10.1523/JNEUROSCI.2578-20.2021.